Investigation on an Integrated Evacuation Route Planning Method Based on Real-Time Data Acquisition for High-Rise Building Fire

Zhuyang Han, Wenguo Weng, Quanlai Zhao, Xin Ma, Quanyi Liu, and Quanyi Huang

***Abstract*—Evacuation of occupants in high-rise buildings is one of the most important tasks when the building is subjected to a significant level of fire threat. Since the mechanism of fire spread is too complicated for the trapped people to determine the evacuation route, a real-time evacuation route planning method is needed for rescue and safety management. In this paper, an integrated real-time evacuation route planning method for high-rise building fires is proposed. This method is composed of real-time data acquisition, risk distribution calculation, and evacuation route formulation. The real-time data acquisition process is achieved by using the sensor system and the wireless data transmission system, the calculation of risk distribution is based on the risk assessment of casualties, and the formulation of evacuation route is based on the fast marching level set method. To demonstrate the presented method, a sample building under an assumed fire is used for numerical investigation, and a real building model is used for experimental investigation. The results show that this method can evaluate the fire status and formulate evacuation strategies instantly in high-rise building fire. The risk distribution and the evacuation route of the building fire can be intuitively displayed. This method can be used in practical applications and will be an important technical basis for the program development of rescue and evacuation.**

***Index Terms*—Evacuation route, high-rise building fire, risk assessment.**

I. Introduction

NOWADAYS, high-rise buildings in the metropolis are rapidly developing. Working in a large construction has become part of modern urban life. However, accidents in high-rise buildings may cause a large number of casualties and economic losses due to the complexity of the architectural structure and the high population density in the building. In particular, fire disasters in high-rise buildings are great threats to urban public safety, since there are so many combustible materials in buildings that lead to rapid combustion and spread of fire. On February 9, 2009, thousands of people were evacuated due to the conflagration at the Cultural Center of China Central Television. On November 15, 2010, the conflagration that happened in Shanghai caused 58 deaths and shocked the whole county. In the U.S., there are more than 20 000 high-rise building fires every year, which induces nearly 1000 casualties and $200 million in losses [1].

The evacuation of occupants is of primary concern when a building is engulfed in an emergency situation caused by a fire accident. An organized evacuation of the occupants from the building is most desired in case of an accidental fire [2]. For 30 years, many significant works has been done on this issue, particularly on the formulation of an evacuation route for protecting people from these disasters. However, these works mainly focus on the formulation of an evacuation route based on the construction layout of the building before the disaster happens. Since evacuation behavior involves both the physical and the behavioral characteristics of crowds, some research on pedestrian flow also takes human behaviors into consideration [3]–[5]. Strategies of feedback control are developed for crowd models to control the movement of people during evacuation from large halls and buildings for mass evacuation [2], [6], [7]. According to the result of a fire evacuation drill, the dynamic changes in evacuation time and the evacuation number of people for each access to the building can be calculated [8]. By using the localization method for wireless sensor network (WSN) nodes, the locations of the trapped persons can be also obtained and used for movement control in evacuation [9], [10].

However, when a fire disaster happens, uncertainties in combustion and smoke propagation complicate the situation, and the previous calculated evacuation route may be incorrect. Hence, the rules and the design principles used for evacuation route planning may not be sufficient enough to explain the complex interaction among a vast number of variables affecting the evacuation process. In addition, the characteristics of a fire disaster would vary in different buildings, which lead to distinctly different behavioral patterns and physiological characteristics of occupants [11]. Recently, two approaches have been also used to represent the buildings in evacuation models: fine and coarse networks [12]. However, neither of these approaches is satisfactory due to the spatial and temporal complexity of large and complex buildings [13].

Since a comprehensive collection of information about the fire is usually impossible, it will be difficult to show trapped people where they should go and for the rescuers to tell what is dangerous and what is safe. Therefore, it is very important

Manuscript received April 25, 2012; revised September 4, 2012; accepted December 25, 2012. Date of publication January 25, 2013; date of current version May 29, 2013. This work was supported in part by the National Basic Research Program of China (973 Program) under Grant 2012CB719705 and in part by the National Natural Science Foundation of China under Grant 51076073 and Grant 91024018. The Associate Editor for this paper was F.-Y. Wang.

The authors are with the Institute of Public Safety Research, Department of Engineering Physics, Tsinghua University, Beijing 100084, China (e-mail: crazyhan@gmail.com; wgweng@tsinghua.edu.cn; iamzql815@gmail.com; thincucumber@126.com; quanyiliu2005@126.com; qyhuang@tsinghua.edu.cn).

Color versions of one or more of the figures in this paper are available online at http://ieeexplore.ieee.org.

Digital Object Identifier 10.1109/TITS.2012.2237398

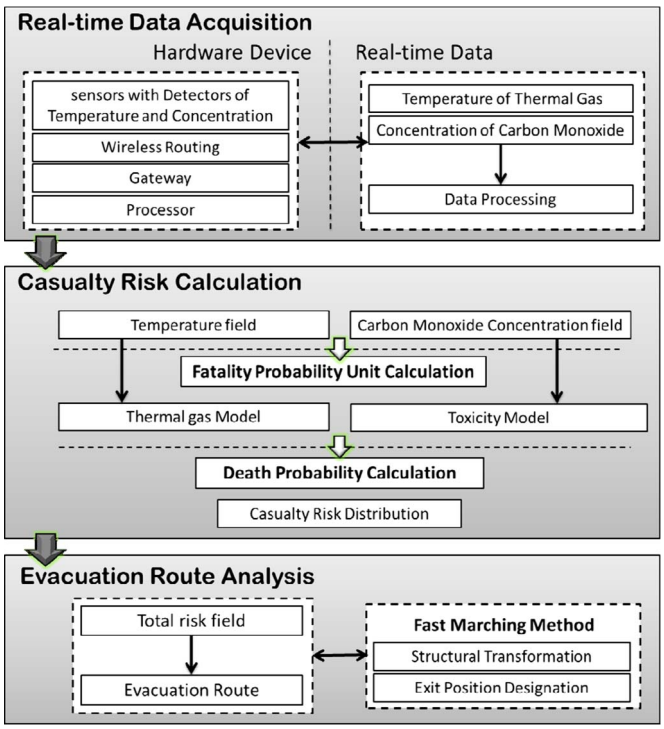

Fig. 1. Framework of the integrated real-time evacuation route planning method.

to instantly evaluate the risk distribution and formulate an evacuation route based on real-time information on the fire [14], [15], which will be of great help to trapped people to escape from fire.

In this paper, an integrated real-time evacuation route planning method for high-rise building fires is proposed. The emphasis of this method is on the real-time data acquisition of temperature and carbon monoxide concentration, which is used to evaluate the status and spread of a fire. In Section II, the proposed method is presented. In Section III, the application of this method is demonstrated by using a sample building for numerical investigation and a real building model for experimental investigation. The results of this method are also discussed in Section III, followed by the conclusions.

II. Method

Here, we propose an integrated real-time evacuation route planning method, including real-time data acquisition, risk distribution calculation, and evacuation route formulation, for a high-rise building fire. The real-time data include temperature of the thermal gas and carbon monoxide concentration of the smoke. The assessment of casualty risk (CR) focuses on the harmful effects of accidents that are fatal to human beings, including high temperature and toxicity of carbon monoxide, which can be obtained by detection devices. The CR is expressed in the form of death probability percentage (DPP). The evacuation route is calculated using the fast marching level set method, which can show the total risk field based on both the risk distribution and the structure of the building. Fig. 1 shows the framework of this method.

A. Real-Time Data Acquisition

The acquisition of real-time data on fire depends on the sensor system and the wireless data transmission system. The sensor system includes detectors of temperature and carbon monoxide concentration. The wireless data transmission system includes a wireless gateway, processors such as computers, and the corresponding software. The real-time data are transmitted under the WSN for emergency event detection and response [16]–[18].

In modern high-rise buildings, there is at least one smoke sensor in each room. These smoke sensors can be refitted by installing the detection devices of temperature and carbon monoxide concentration inside these sensors. The chip of the device used in this work is the improved CC2431 and CC2520 from Texas Instruments. In each room, the detection devices can be installed at any location on the ceiling, which makes the distribution of detectors flexibly enough to fit the requirements of data acquisition. When the sensors work, the sampling periods of all the detectors are set to 2 s. A higher sampling frequency has better timeliness of digital signal, which is the technological foundation of this real-time method.

For need of data transmission, a wireless communication module is also installed inside each sensor [19]. When the transmission system starts to work, a wireless communication environment is established by the controller of this system. Then, each sensor participates in this wireless communication environment in turns and obtains a network address assigned by the controller. Since the sensors cannot participate in the wireless communication environment at the same time, the synchronization of this wireless communication network becomes extremely important. In this paper, the flooding time synchronization protocol method is used for time synchronization of mesh-connected WSNs [20]–[22]. By calibrating the slave nodes with the master node, the clock skew can be quantitatively calculated, and high-precision synchronization can be achieved.

To avoid channel collision in periodic data collection, a synchronization transmission scheme with a cycle time slot is used in this method [23], [24]. This synchronization transmission scheme assigns the transmission process at different moments and reduces the nodes in the same collision domain and the collision probability. In the transmission process, the communication protocol is developed based on the wireless communication protocols of IEEE 802.15.4 [25]. The software of the protocol stack is developed by using the C/C++ cross-compiler of IAR Embedded Workbench [26]. Then, the processors convert the received data for need of risk calculation. When the real-time data are transmitted to the processors, the Kalman filter method is used in this work to filter out the singular values of the data. Fig. 2 shows a refitted sensor with detectors of temperature and carbon monoxide concentration.

B. Risk Calculation

Since the real-time data acquired are the temperature and carbon monoxide concentration at the position of the sensors, it is very important to calculate the temperature and carbon monoxide concentration fields in the building by the interpolating

Fig. 2. Refitted transducer with detectors of temperature and carbon monoxide concentration. (a) Top view of a sensor. (b) Internal view of a sensor (with detectors).

method. For convenience of calculation, the least squares method is used in this work. For the small rooms that have just one sensor, the data acquired by the sensor can be used as the value for the whole room.

After the interpolation calculation of temperature and carbon monoxide concentration fields, the CR distribution can be evaluated. To quantitatively demonstrate the level of damages, fatality probability unit P_T is defined as a mathematical function based on the physiological dose–effect relationship between the dose of harm such as toxicity or heat and the effects of the recipient such as deaths or injuries [27], [28]. The fatality probability unit can be used for the measurement of the damage from an accident; this is the critical basis of the calculation of DPP, which is the final result of the accident consequence.

The fatality probability unit from an accident can be estimated by the following equation [27], [28]:

$$P_T = a + b \ln I_f \tag{1}$$

where a and b are empirical constants that reflect the hazard specific to a harmful load studied and the susceptibility of recipients to the load, respectively. I_f is a dose of the load for a given exposure time. For different accidents and harm, the values of the parameters are different.

For the fatality of the toxicity of carbon monoxide, the relationship between carbon monoxide concentration and the fatality probability unit can be expressed as the following equation [2]:

$$P_T = a + b \ln(C \cdot t) = -37.98 + 3.7 \ln(C \cdot t) \tag{2}$$

where C is the concentration of carbon monoxide (in parts per million), and t is the time of the target exposed to the toxic gas (in seconds). The results calculated by this equation meet with the empirical relationship by experiment [29].

For the fatality of thermal gas, there are no general methodologies for the calculation of thermal gas damages to human beings. Based on the Cranee formula, the relationship between the temperature of thermal gas and the fatality probability unit can be expressed as the following equation [30], [31]:

$$P_T = -21.4214 + 1.5035 \ln\left[(T - 273)^{3.61} \times t_1\right] \tag{3}$$

where T is the temperature of thermal gas (in Kelvin), and t_1 is the time of the target exposed to the thermal gas (in minutes).

By using the fatality probability unit, the DPP of each effect can be obtained by looking up the corresponding table [29].

In this paper, the results of the risk calculation of the building fire are estimated by integrating the harmful effects of high temperature and toxicity of thermal gas. Here, the concept of CR is used. CR is the probability of a person dying in an accident, which is calculated by adding the DPP of high temperature and toxicity of carbon monoxide. The minimum value of fatality probability unit P_T is 0, and the maximum value of the CR is 100%.

C. Evacuation Route Analysis

For the trapped persons who want to run out of the building on fire, the evacuation route should not only follow the gradient of the CR field but consider the exits of the building as well. Hence, the CR distribution and the architectural structure of the building should be integrated together to show the risk distribution of the building fire. In this paper, the concept of "total risk" is used as the integrated risk, in which the location of all the exits, the distance between the exits and the human, and the CR distribution are combined. The fast marching level set method is chosen as the method to calculate the total risk distribution. By solving the gradient equations, the total risk distribution can be obtained, which also indicates the final risk distribution for the formulation of the evacuation route.

For the total risk distribution in the building, the total risk at all the exits of the building should be the lowest because exits are the closest place to the safe area. The risks at the exits should be first set, and the gradient of the total risk field should be toward the building's closest exit. Then, the solving formula of the total risk can be expressed in the form of the Eikonal equation [32]–[35]. The fast marching level set method, which is a numerical scheme for computing solutions to the nonlinear Eikonal equation and related static Hamilton–Jacobi equations, is presented here for monotonically advancing fronts. Based on entropy-satisfying upwind schemes and fast sorting techniques, they yield consistent, accurate, and highly efficient algorithms [33]. The fast marching method is a numerical algorithm for solving the Eikonal equation on a rectangular orthogonal mesh in O(MlogM) steps, where M is the total number of grid points [35]. This method has been widely used in fields about optimal path planning [33]. In this paper, since data acquisition and risk calculation are both 2-D, the Eikonal equation used for solving the total risk distribution can be expressed as [32]–[35]

$$|\nabla T| F = \frac{|\nabla T|}{\mathrm{R}} = 1 \tag{4}$$

where R is the CR field for each grid point, and F is the reciprocal of R, i.e., $F = 1/R$ and is typically supplied as known input to the equation. T is the total risk field.

Before using the fast marching level set method to solve (4), the study area and the CR field of the building should be discretized and converted to a rectangular grid. After the discretization of CR field R, (4) can be expressed as follows for solving [32]:

$$\frac{1}{F^2} = \max\left(D_{ij}^{-x}T, 0\right)^2 + \min\left(D_{ij}^{+x}T, 0\right)^2 + \max\left(D_{ij}^{-y}T, 0\right)^2 + \min\left(D_{ij}^{+y}T, 0\right)^2 \tag{5}$$

where D_{ij}^{-} is the forward operator at matrix grid point (i,j), and D_{ij}^{+} is the backward operator at matrix grid point (i,j), which can be expressed as follows [32]:

$$\begin{cases} T(x,y,0)=0 \\ D_{ij}^{-x}T=\frac{T_{ij}-T_{i-1,j}}{x_i-x_{i-1}} \\ D_{ij}^{+x}T=\frac{T_{i+1,j}-T_{ij}}{x_{i+1}-x_i} \\ D_{ij}^{-y}T=\frac{T_{ij}-T_{i,j-1}}{y_j-y_{j-1}} \\ D_{ij}^{+y}T=\frac{T_{i,j+1}-T_{ij}}{y_{j+1}-y_j} \end{cases} \tag{6}$$

where x_i and y_i are the coordinate values of the x and y coordinates at matrix grid point (i,j), respectively.

When solving the Eikonal equation, the grid points are divided into three kinds: alive point, narrow-band point, and far away point. Alive point is the point of which the total risk value is known and unchanged. The narrow-band point is the point that is near the alive point. There should be at least one alive point near a narrow-band point. The other points are a far away point of which the total risk value is unknown and of which there are no alive points nearby.

In solving (4), the total risk of the grid point at the exit of the building is set to 0. That is the lowest total risk value in the building, and these grid points are alive points. For the grid points of narrow band near the exit, the total risk value can be obtained by solving (5). By using an iteration and circulation algorithm, the total risk values at all the grid points can be solved.

The detailed solving process of the fast marching level set method to (4) is presented as follows [32]:

1) Initialize
   (a) Initialization of alive points: Let alive points be the set of all grid points at the exit of the building; set $T_{i,j}=0$ for all the alive points.
   (b) Initialization of narrow-band points: Let narrow-band points be the set of all grid points near the exit (near the alive points); set $T_{i,j}=dy/F_{ij}$ for all the narrow-band points.
   (c) Initialization of far away points: Let far away points be the set of all the other grid points; set $T_{i,j}=\infty$ for all the far away points.
2) Marching Forward
   (a) Begin Loop: Let $(i_{\min},j_{\min})$ be the point in narrow-band point with the smallest value of T.
   (b) Add the point $(i_{\min},j_{\min})$ to alive point and remove it from narrow-band point.
   (c) Tag as neighbors any point $(i_{\min}-1,j_{\min})$, $(i_{\min}+1,j_{\min})$, $(i_{\min},j_{\min}-1)$, or $(i_{\min},j_{\min}+1)$ that is either in narrow-band point or in far away point. If the neighbor is far away point, remove it from that list and add it to the set of narrow-band point.
   (d) Recompute the values of T at all neighbors according to (5), selecting the largest possible solution to the quadratic equation.
   (e) Return to the top of this Loop.

More information about the calculation process can be found in [32]. It is shown that the key to solving the problem is in the selection of grid point in the narrow-band point to update [32]. By solving these equations in matrix grid, total risk field T can be obtained. The evacuation route can be formulated by following the gradient of the total risk field.

The spatial layout and structure of the building should be investigated first, when using the integrated real-time evacuation route planning method previously proposed. Moreover, the sensors of temperature and carbon monoxide concentration and the wireless data transmission system should be installed in each room. After that, by using the proposed method, the algorithm can get the required data and calculate the risk distribution. According to the correspondence between the rooms and the sensors, the distribution of temperature, carbon monoxide concentration, and CR can be obtained for the whole building. For each room, sensors may acquire data for risk analysis, and the risk of the whole building can be gained by integrating the risks of all the rooms.

In particular, in this paper, the architectural structure and the CR distribution of the building are combined as the total risk distribution, and the gradient of the total risk field is toward the closest safe exit of the building. Hence, the selection of the exits is to follow the gradient of the total risk field and reach the closest safe exit. For a different building, the number of the rooms and the complexity of the building structures do not affect the feasibility of the method, and the application of this method does not rely on the spatial layout and building structure.

III. Applications and Discussions

Here, we validate the method proposed in Section II by using a sample building and a real building model with a scale of 1 : 20. For numerical investigation, the sample building is used, which is a part of a real building on the fourth floor. For experimental investigation, the real building model with three floors is used. These investigations also show how the proposed method is used in application.

These two buildings that are not big architectures are chosen to improve display accuracy and reduce computational complexity since the method proposed here does not rely on the building structure. Detailed information on the sample buildings and the analysis process are presented to demonstrate the application of the method. For the application of big architectures, the only difference is to change the building structure.

A. Real Sample Building for Numerical Investigation

The sample building used here is a part of a building at Tsinghua University, Beijing, China. The length of the building is 25.9 m, the width is 14.9 m, and the height is 3 m. It contains ten rooms and two connected corridors. Fig. 3 shows the structure of this building. The rooms are numbered from 1 to 8 and 11 and 12. The corridors are numbered 9 and 10. The exit of this building is located at the end of corridor 10. All the doors are also shown in Fig. 3(a). In this application, an assumed

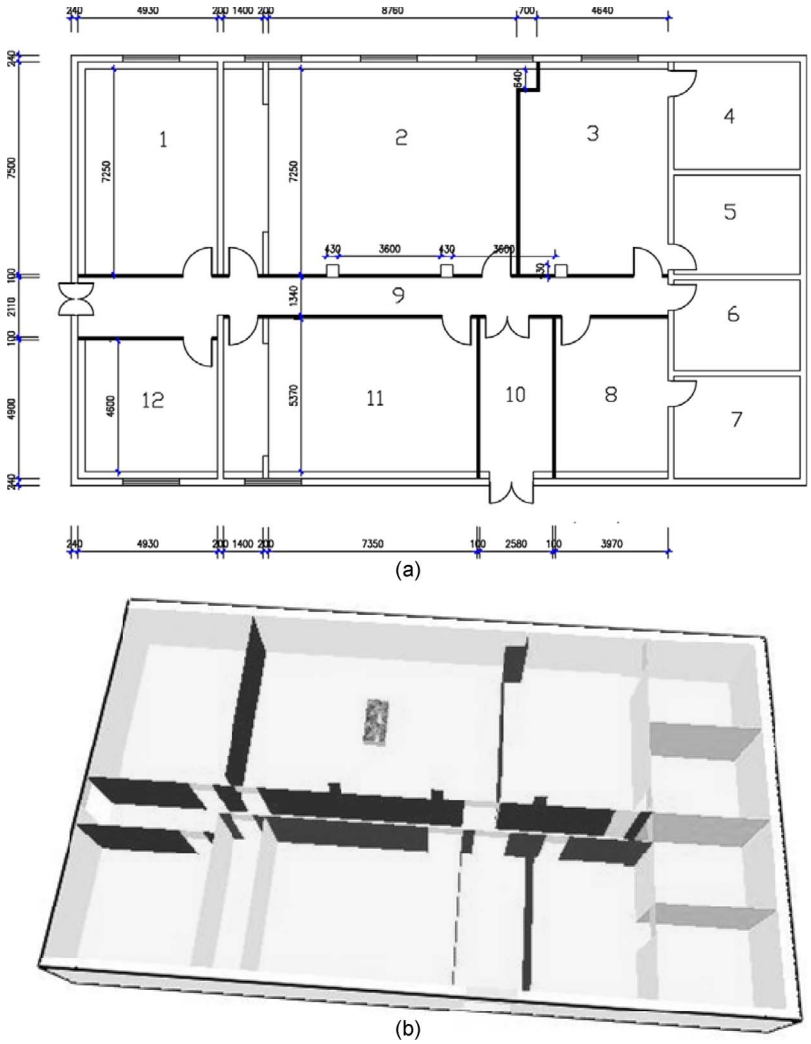

Fig. 3. Structure of the sample building. (a) Structure of the sample building by CAD. (b) Three-dimensional model of the sample building with the initial assumption of the fire.

fire is set in the sample building. The Fire Dynamics Simulator (FDS), which is a computational fluid dynamics model of fire-driven fluid flow [36]–[38] that has been developed by the National Institute of Standards and Technology of the U.S. Department of Commerce, is used to simulate the spread of fire with the assumed fire. The results of FDS simulation are used as the status of the assumed fire disaster for casualty risk calculation and evacuation route analysis.

It is assumed that there is only one sensor in each room and corridor. The chosen locations of all the sensors are shown in Table I. All of the sensors are on the ceiling of the rooms.

The initial assumption of the fire is listed as follows,

a) The fire source is located in the middle of room 2, as shown in Fig. 3(b).
b) The combustion mode of the fire source is incomplete combustion. Much carbon monoxide may be generated in the smoke and be transmitted in the building.
c) All the doors in the building are kept open. The ventilation in the rooms is good.
d) During the simulation, all the sensors are normally operating.

TABLE I
POSITION OF THE SENSORS IN THE SAMPLE BUILDING FOR THE NUMERICAL INVESTIGATION

No. of sensor	X-Coordinate (m)	Y-Coordinate (m)	Z-Coordinate (m)
1	3.03	11.39	3.00
2	9.10	10.25	3.00
3	16.90	11.39	3.00
4	23.40	14.43	3.00
5	22.97	9.11	3.00
6	24.27	6.46	3.00
7	22.10	2.66	3.00
8	11.70	6.84	3.00
9	19.50	3.42	3.00
10	16.47	4.56	3.00
11	12.57	4.56	3.00
12	3.03	2.66	3.00

According to the spatial layout structure of the building and the locations of the sensors, as shown in Fig. 3(a) and Table I, the aforementioned method can be used for risk assessment and evacuation route planning.

TABLE II
TEMPERATURE AND CARBON MONOXIDE CONCENTRATION AT THE CHOSEN POSITIONS FOR THE NUMERICAL INVESTIGATION

No.	t=30s		t=60s		t=90s		t=120s		t=150s	
	T (°C)	CO (ppm)	T (°C)	CO (ppm)	T (°C)	CO (ppm)	T (°C)	CO (ppm)	T (°C)	CO (ppm)
1	20	0	41.344	2308.2	78.181	7535.9	94.045	10888.0	102.180	13348.0
2	56.12	2905.7	166.88	13073.0	209.54	18381	233.32	20486.0	216.78	19329.0
3	20	0	40.991	2233.1	78.026	7473.1	78.119	9616.4	99.327	12876.0
4	20	0	20	0	32.570	1518.6	42.568	4181.6	50.884	6693.6
5	20	0	20	0.2	23.051	444.98	31.808	2003.9	39.887	3806.7
6	20	0	28.582	957.8	44.362	3587.4	55.726	6367.3	62.227	8519.9
7	20	0	20	0	20	1	22.556	423.6	26.467	1315.1
8	20	0	46.165	2787.5	91.313	9714.4	99.649	13219.0	103.63	14497.0
9	20	0	20	0	26.109	810.41	34.8	2463.1	40.715	3896.5
10	20	0	25.333	534.3	46.568	3345.8	62.343	6236.6	69.154	8131.5
11	20	0	23.436	349.1	39.477	2608.3	58.147	6185.6	63.665	7621.2
12	20	0	20	0	26.043	767.34	36.741	2540.2	45.399	4461.9

TABLE III
FATALITY PROBABILITY UNIT P_T, THE DPP, AND THE CR FOR THE NUMERICAL INVESTIGATION

Time	Risk	1	2	3	4	5	6	7	8	9	10	11	12
	P_T (T)	0	5.55	0	0	0	0	0	0	0	0	0	0
	P_T (CO)	0	4.11	0	0	0	0	0	0	0	0	0	0
t=30s	DPP (T)	0.23	0.72	0.23	0.23	0.23	0.23	0.23	0.23	0.23	0.23	0.23	0.23
	DPP (CO)	0	0.19	0	0	0	0	0	0	0	0	0	0
	CR	0	0.91	0	0	0	0	0	0	0	0	0	0
	P_T (T)	3.89	11.47	3.85	0	0	1.89	0	4.49	0	1.24	0.81	0
	P_T (CO)	3.26	9.67	3.14	0	0	0	0	3.96	0	0	0	0
t=60s	DPP (T)	0.13	1	0.13	0	0	0	0	0.31	0	0	0	0
	DPP (CO)	0.04	1	0.04	0	0	0	0	0.15	0	0	0	0
	CR	0.17	1	0.17	0	0	0	0	0.46	0	0	0	0
	P_T (T)	7.35	12.70	7.34	2.60	0.72	4.28	0	8.19	1.40	4.54	3.64	1.39
	P_T (CO)	7.64	10.93	7.60	1.71	0	4.89	0	8.58	0	4.63	3.71	0
t=90s	DPP (T)	0.99	0.99	0.99	0	0	0.24	0	1	0	0.33	0.09	0
	DPP (CO)	0.99	0.99	0.99	0	0	0.46	0	1	0	0.36	0.1	0
	CR	1	1	1	0	0	0.7	0	1	0	0.69	0.19	0
	P_T (T)	8.35	13.29	7.35	4.05	2.47	5.51	0.60	8.67	2.96	6.12	5.74	3.25
	P_T (CO)	9.00	11.34	8.54	5.46	2.73	7.01	0	9.72	3.50	6.94	6.91	3.61
t=120s	DPP (T)	1	1	0.99	0.17	0	0.7	0	1	0.02	0.87	0.78	0.05
	DPP (CO)	1	1	1	0.68	0.02	0.98	0	1	0.07	0.98	0.98	0.09
	CR	1	1	1	0.85	0.02	1	0	1	0.09	1	1	0.14
	P_T (T)	8.80	12.89	8.65	5.02	3.70	6.11	1.47	8.88	3.81	6.69	6.24	4.40
	P_T (CO)	9.75	11.12	9.62	7.20	5.11	8.09	1.18	10.06	5.20	7.92	7.68	5.70
t=150s	DPP (T)	1	1	1	0.51	0.1	0.87	0	1	0.12	0.96	0.9	0.28
	DPP (CO)	1	1	1	0.99	0.55	1	0	1	0.58	1	0.99	0.7
	CR	1	1	1	1	0.65	1	0	1	0.8	1	1	0.98

For data acquisition, the results of FDS simulation are used as the status of the assumed fire disaster. At the positions chosen as the locations of the sensors, the results of temperature and carbon monoxide concentration calculated by FDS are used as the detected value of the sensors. These values are shown in Table II and can be used as the database of CR calculation and evacuation route analysis.

For the risk calculation, since all the rooms are small with just one sensor, the data previously acquired can be used as the value for the whole room. Hence, the data shown in Table II can be used in the CR calculation for each room. For the assessment of the harmful effects of high temperature and toxicity of carbon monoxide, (2) and (3) can be used, respectively. The calculation results are shown in Table III. The DPP of these two harmful effects can be obtained by looking up the corresponding table [29], and the results are also shown in Table III. The CR can be estimated by adding the DPP of high temperature and toxicity of thermal gas. The results of risk assessment are

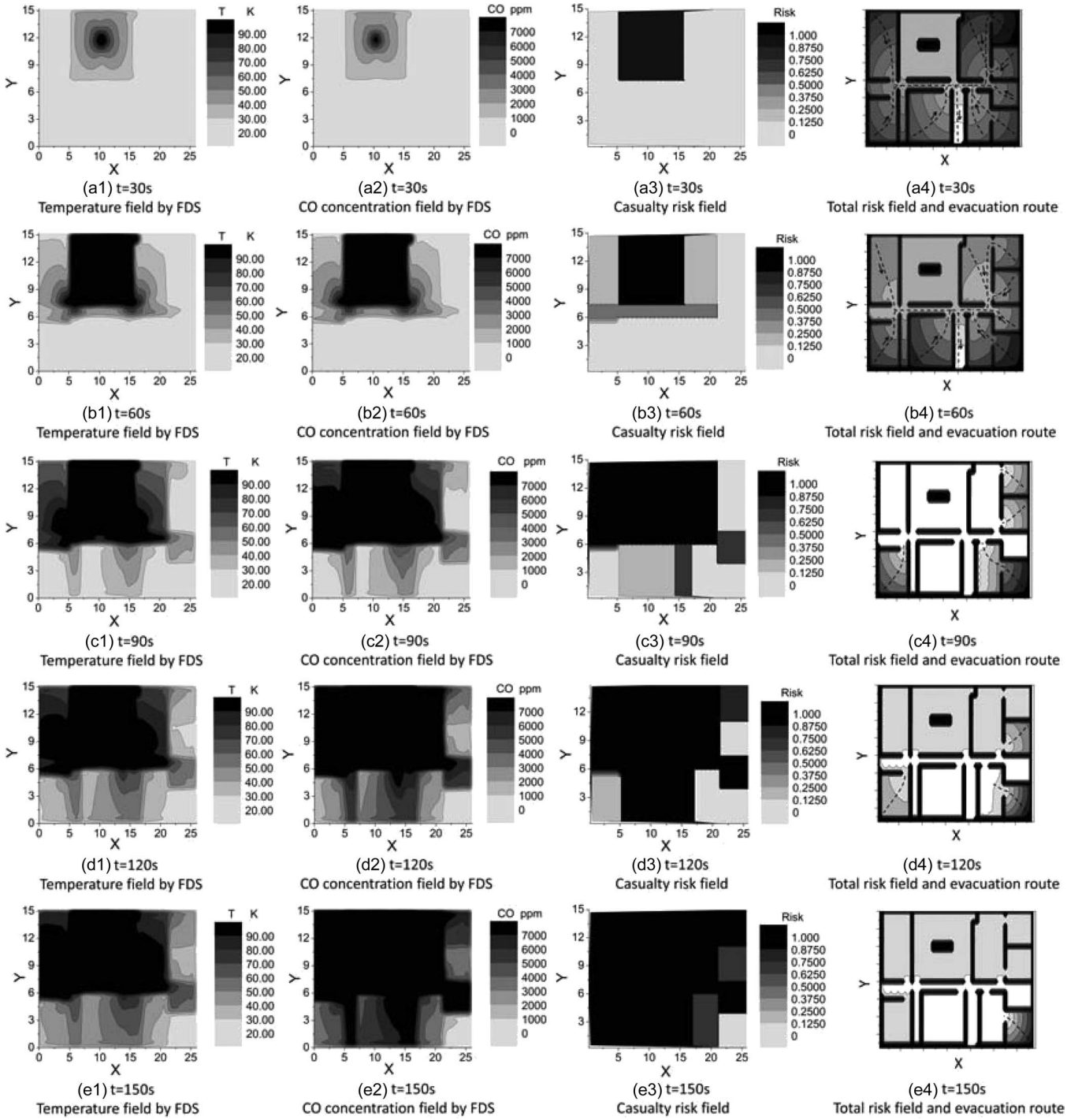

Fig. 4. Results of FDS simulation, CR calculation, and evacuation route analysis for the sample building. (a) $t = 30$ s. (b) $t = 60$ s. (c) $t = 90$ s. (d) $t = 120$ s. (e) $t = 150$ s.

shown in Fig. 4(a3), (b3), (c3), (d3), and (e3), and Table III shows the calculation results of fatality probability unit P_T, the DPP, and the CR at the locations of the sensors in the numerical investigation. It should be noticed that the recommended value of the exposure time for people referred to high temperature and toxicity of carbon monoxide is assumed at 30 s [39].

For the evacuation route analysis, the CR distribution is integrated with the architectural structure of the building using the fast marching level set method. The results of total risk distribution and evacuation route analysis are shown in Fig. 4.

As shown in Fig. 4(a)–(e), the results of calculation and analysis clearly displayed the diffusion of thermal gas. The temperature and carbon monoxide concentration in room 2 are apparently higher than in other rooms during the experiment, since the fire source is located in the middle of room 2, as shown in Fig. 4(a1), (a2), (b1), and (b2) and Table II. When $t = 30$ s, the combustion heats the surrounding air, raises the temperature in room 2, and releases thermal gas that is mixed with carbon monoxide, which is shown in Fig. 4(a1) and (a2). The CR in room 2 is very high; hence, room 2 is not safe for

human occupancy. Other rooms are not affected yet because the duration of the combustion is too short for thermal gas to spread, as shown in Fig. 4(a3). Therefore, at this time, most of the rooms and areas in this building are safe, and it will be feasible for people to evacuate, as shown in Fig. 4(a4). When $t = 60$ s, the combustion continues, and more thermal gas are released. The thermal gas begins to spread, and the diffusion airflow reaches corridor 9 and the areas close to the opening doors in rooms 1 and 3. The temperature and carbon monoxide concentration of corridor 9 keep increasing, as shown in Fig. 4(b1) and (b2). In Fig. 4(b3), it is shown that room 2 becomes fatal with a CR of 1 (DPP is 100%), and the CR in corridor 9 also increases. Since corridor 9 is not fatal yet (the CR < 1), it is still possible for people to escape from the building, as shown in Fig. 4(b4). When $t = 90$ s, the thermal gas continues to diffuse. The diffusion airflow keeps getting into rooms 1 and 3 and reaches rooms 6 and 11 by the doors, which is shown in Fig. 4(c1) and (c2). At this time, rooms 1 and 3 and corridor 9 are all full of toxic thermal gas with a CR of 1, as shown in Fig. 4(c3), which means that corridor 9 is not safe and cannot be used for evacuation, as shown in Fig. 4(c4). Therefore, in that case, it is not possible for trapped people to run out of the building from rooms 4, 5, 7, 8, and 12. For the trapped people in these areas, they should stay in the room, close the door, and wait for rescue. In particular, when $t = 120$ s, rooms 1, 3, 6, and 11 and corridor 9 are all full of toxic thermal gas, and room 4 also gets involved, as shown in Fig. 4(d1) and (d2). Hence, now, only rooms 5, 7, and 12 are not fatal for people to evacuate. The only chance for the trapped people to survive is to stay inside and wait for rescue, as shown in Fig. 4(d3) and (d4). Finally, when $t \geq 150$ s, most parts of the building have a CR of 1 (DPP is 100%), which means that all these parts of the building are fatal, as shown in Fig. 4(e1)–(e4).

By comparing the figures of different time, the calculation results of the CR and total risk fields can also display the risk distribution and the diffusion process of thermal gas in the whole building area. Hence, the analysis result of the evacuation route will be helpful for people in knowing which place is safe. From the calculation results of the CR field, it is shown that the thermal gas gradually diffuses from room 2 to the long corridor 9 and then to rooms 1, 3, 6, and 11 and corridor 10. Therefore, the CRs in these areas are higher than in other areas, as shown in Fig. 4(b3), (c3), and (d3). However, the CR field cannot accurately show the risk distribution in each room. That is because there is only one sensor in each room, and the results of interpolation calculation are not accurate enough to reflect the distribution of temperature and carbon monoxide concentration. For the evacuation route analysis, as shown in Fig. 4(a4), (b4), (c4), (d4), and (e4), the gradient of the total risk field of each room is always toward the door and the exit of this building. Hence, the evacuation route can follow the gradient direction of the total risk field and show the safest route to escape from the fire. In Fig. 4(a4) and (b4), the evacuation routes are clearly plotted, which means people can escape from the building by following these routes. In Fig. 4(c4), (d4), and (e4), many rooms and corridors in the building are fatal with a CR of 1; hence, there are no complete routes in these cases, and it is not possible for the trapped people to run out of the building.

These analyses results indicate that the proposed method can be applied to the risk assessment of building fire and the formulation of an evacuation route. The result of the CR calculation can intuitively display the risk distribution in the building. The evacuation route can be formulated based on the CR distribution and the architectural structure of the building. The accuracy of the risk distribution depends on the number of sensors in each room. More sensors mean better calculation accuracy. In practical applications, the risk distributions in small rooms are not necessary for the formulation of the evacuation route of the whole building. For large areas, such as a large conference room, theater, and cinema, more sensors should be installed for better formulation of the evacuation route.

B. Real Building Model for Experimental Investigation

The real building model with a scale of $1:20$ used here has three floors, five rooms, and two stairwells. The length of this model is 48 cm, the width is 32 cm, and the height is 45 cm. The height of each floor is 15 cm. Each room is connected to at least one room or stairwell nearby. Fig. 5 shows the structure of this building. The rooms are numbered 1, 2, 5, 8, and 9, in which room 5 is divided into two parts by a bearing wall, as shown in Fig. 5(b). Areas 3 and 4 are a stairwell, and areas 6 and 7 are another stairwell. The exit of this building is located at the edge of room 1, as shown in Fig. 5(a). All the doors are also shown in Fig. 5(a)–(c). Ten sensors integrated detection devices of temperature and carbon monoxide concentration are placed in the building model, as shown in Fig. 5(e). The positions of the sensors are shown in Table IV. This real building model is made of asbestos board; hence, it is noncombustible but a good conductor of heat.

In this experiment, the combustible materials are some papers with alcohol. The fire source is located in room 5, which is next to the seventh sensor. Since asbestos is noncombustible, the fire does not overspread to other areas of the building model. All the doors in this building model are kept open; hence, thermal gas can be transmitted through the doors among different rooms. The temperature of the environment is 19.02 °C. Based on the spatial layout structure of the building and the locations of the sensors, as shown in Fig. 5 and Table IV, the evacuation route planning method can be used in this experimental investigation.

For the data acquisition, the data are acquired by the sensors and recorded in a computer during the experiment. In application, the temperature and carbon monoxide concentration can be detected by the sensors and recorded every 2 s. For the risk analysis in the next step, three sets of data at $t = 120$, 180, and 320 s are chosen, as shown in Table V.

For the risk calculation, since each room has one sensor, the data previously acquired can be used as the value for the whole room. Hence, the data shown in Table V can be used in the CR calculation for each room. Then, (2) and (3) can be used for the assessment of the harmful effects of high temperature and toxicity of carbon monoxide, respectively. The calculation results are shown in Table VI. The DPP of these two harmful effects can be obtained by looking up the corresponding table [29], and the results are also shown in Table VI. The CR can be

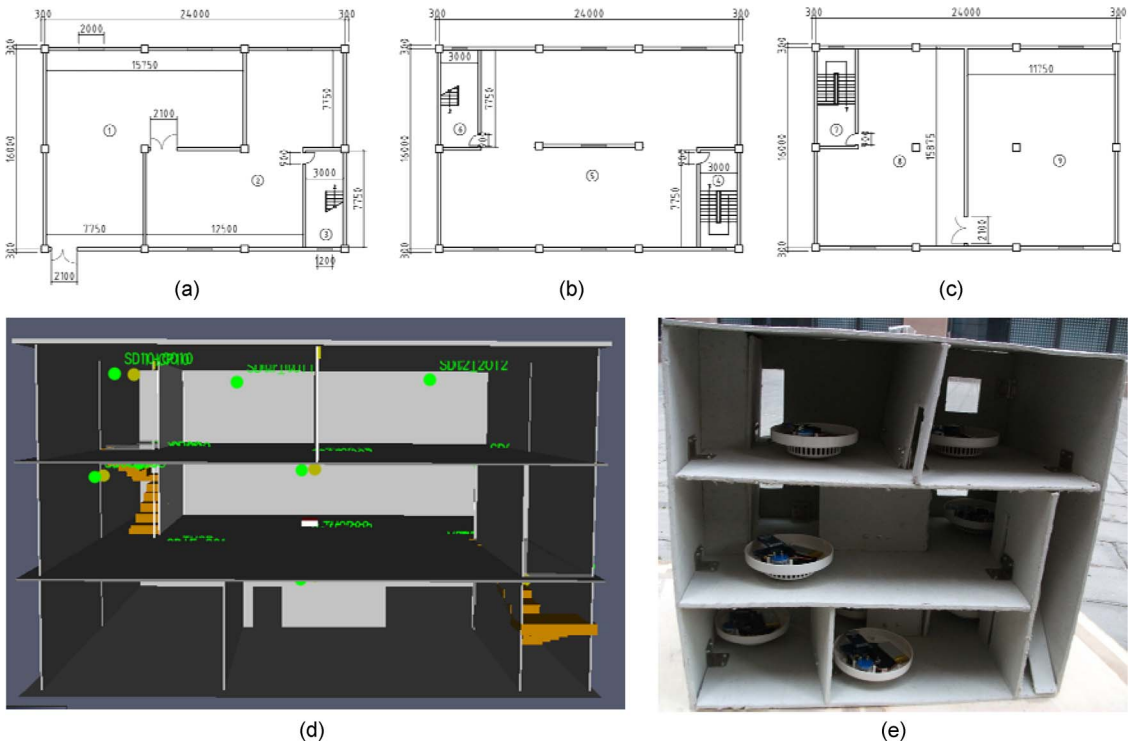

Fig. 5. Structure of the real building model. (a) First floor structure by CAD. (b) Second floor structure by CAD. (c) Third floor structure by CAD. (d) Three-dimensional model with inner walls hidden. (e) Side view of the building model with sensors installed.

TABLE IV
POSITION OF THE SENSORS IN THE REAL BUILDING MODEL FOR THE EXPERIMENTAL INVESTIGATION

No. of transducer	X-Coordinate (cm)	Y-Coordinate (cm)	Z-Coordinate (cm)
1	8	8	3
2	16	24	3
3	29	8	3
4	40	24	3
5	45	8	15
6	35	24	18
7	31	8	18
8	3	24	30
9	15	16	33
10	36	16	33

TABLE V
ACQUIRED DATA OF THE SENSORS IN THE REAL BUILDING MODEL FOR THE EXPERIMENTAL INVESTIGATION

No.	t=120s		t=180s		t=320s	
	T (°C)	CO (ppm)	T (°C)	CO (ppm)	T (°C)	CO (ppm)
1	20.03	42	21.02	78	23.00	110
2	22.02	36	23.02	119	24.03	147
3	20.02	32	21.00	125	21.03	158
4	18.00	68	18.01	308	18.03	203
5	19.02	143	20.00	249	20.02	34
6	27.01	626	32.01	1809	44.02	2431
7	31.02	1350	40.01	2534	59.02	3308
8	26.03	1445	31.03	5731	46.01	6816
9	27.00	2573	34.00	6762	52.03	8190
10	19.02	879	26.03	3436	33.01	4765

estimated by adding the DPP of high temperature and toxicity of thermal gas. The results of risk assessment are shown in Fig. 6(a1), (b1), and (c1), and Table VI shows the calculation results of fatality probability unit P_T, the DPP, and the CR in the experimental investigation. The recommended value of the exposure time for people referred to high temperature and toxicity of carbon monoxide is assumed at 30 s [39].

For the evacuation route analysis, the exit of the building is located at the front door on the first floor. By using the fast marching level set method, the total risk field can be calculated by integrating the CR distribution and the architectural structure of the building. The results of evacuation route analysis are shown in Fig. 6.

For convenience of displaying the complete evacuation route, all of the three floors of the building are combined, as shown in Fig. 6. The second floor is horizontally flipped and connected to the first floor from the left side and the third floor from the right ride, which means that areas 3 and 4, which belong to the same stairwell, are connected in Fig. 6, as are areas 6 and 7. Hence, the total risk field can be comprehensively shown from the top view, and it will be easier to see the evacuation route from the third floor to outside. As shown in Fig. 6(a)–(c), three floors of the building are connected and shown as one structure diagram. The risk distributions of the three floors are combined, which makes it better to show the evacuation route from the third floor to the first floor.

In Fig. 6(a1), (b1), and (c1), the calculation results of the CR field show the risk distribution and spread process of fire in the whole building area. When $t = 120$ s, there is no obvious change in the CR field, as shown in Fig. 6(a1), since the combustion is not intense. When $t = 180$ s, the area close to the

TABLE VI
FATALITY PROBABILITY UNIT P_T, THE DPP, AND THE CR FOR THE EXPERIMENTAL INVESTIGATION

Time	Risk	1	2	3	4	5	6	7	8	9	10
t=120s	P_T (T)	0	0.47	0	0	0	1.58	2.33	1.38	1.58	0
	P_T (CO)	0	0	0	0	0	0	1.27	1.53	3.66	0
	DPP (T)	0	0	0	0	0	0	0	0	0.01	0
	DPP (CO)	0	0	0	0	0	0	0	0	0.09	0
	CR	0	0	0	0	0	0	0	0	0.1	0
t=180s	P_T (T)	0.22	0.72	0.22	0	0	2.50	3.72	2.34	2.83	1.38
	P_T (CO)	0	0	0	0	0	2.36	3.60	6.62	7.24	4.73
	DPP (T)	0	0	0	0	0	0	0.1	0	0.02	0
	DPP (CO)	0	0	0	0	0	0	0.09	0.95	0.99	0.4
	CR	0	0	0	0	0	0	0.19	0.95	1	0.4
t=320s	P_T (T)	0.71	0.95	0.22	0	0	4.23	5.83	4.47	5.14	2.67
	P_T (CO)	0	0	0	0	0	3.45	4.59	7.26	7.94	5.94
	DPP (T)	0	0	0	0	0	0.23	0.8	0.3	0.56	0.01
	DPP (CO)	0	0	0	0	0	0.06	0.34	0.99	1	0.83
	CR	0	0	0	0	0	0.29	1	1	1	0.84

fire source in room 5 has a higher temperature than other areas, which leads to the increase in CR in room 5. In addition, the smoke produced in the incomplete combustion process moves upward through stairwell 6 and 7 to room 8 on the third floor. There is a significant change in carbon monoxide concentration in stairwell 6 and 7 and room 8. The CR is rapidly increased in these areas, which is shown in Fig. 6(b1). When $t = 320$ s, the thermal gas continues to spread and move upward, which leads to the increase in temperature and carbon monoxide concentration in rooms 5 and 9. The fast increase in temperature in room 8 is due to the heat transfer by conduction through the asbestos board on the ceiling of the second floor. The risks in this building model keep increasing, except on the first floor, as shown in Fig. 6(c1). Hence, the exit of the building is still safe enough to escape.

Fig. 6(a2) shows the evacuation route when $t = 120$ s, which depicts that the fire on the second floor is not intensive, and room 5 is not fatal. Hence, the trapped people can escape from the third floor to the exit of the building by following the evacuation route. When $t = 180$ s, only rooms 1, 2, and 5 and stairwell 3 and 4 can be used for evacuation. The evacuation route is shown in Fig. 6(b2), from the second floor to the first floor. At that time, stairwell 6 and 7 and room 8 are fatal with a CR of 1, which means that these areas are not safe for people to evacuate. Therefore, it is impossible for the trapped people on the third floor to run out of the building. Since room 9 is safer than room 8, people in room 9 should stay in the room and wait for rescue. When $t = 320$ s, most areas on the second and third floors have a CR of 1; hence, the evacuation route starts from stairwell 4 to the exit of the building on the first floor, as shown in Fig. 6(c2).

The analysis results of the real building model in the experimental investigation can be also compared with the calculation results by using FDS. In FDS, it is assumed that the heat release rate of the fire source is linearly increased in the first 200 s of the combustion and then maintains at 1.5 MW. The calculation results by FDS and the data measured in the experiment are shown in Fig. 7, including the calculation values and measured data of temperature and carbon monoxide concentration at the location of sensors 2, 7, and 9. Sensors 2, 7, and 9 are on the first, second, and third floor, respectively. These results can be also used to demonstrate the temperature and carbon monoxide concentration value on the three floors, respectively. In Fig. 7(a), according to the FDS simulation results, it is shown that the temperatures on the three floors keep on increasing, and the temperature on the second floor near the fire source is significantly higher than that on the first and third floor. With the combustion progress, the temperature on the third floor is also gradually increasing and becomes dangerous, but the first floor is still safe. These trend and relationship are similar with the data measured in the experiment. The highest temperature is detected on the second floor of sensor 7, and the lowest temperature is on the first floor of sensor 2. The temperature of sensors 7 and 9 keeps increasing, but it has no apparent change on the first floor. Fig. 7(b) shows that the carbon monoxide concentrations on the three floors have the same trend as the temperature distribution. The second floor is significantly fatal because of the aggregation of toxic gas produced in the combustion process. The third floor becomes extremely hazardous due to the rising effects of the airflow from the second floor through stairwell 6 and 7. It is also shown that the first floor is always safe with the toxic gas hardly falling down through stairwell 3 and 4. Similarly, from the measurement data in the experiment, the carbon monoxide concentration on the third floor is significantly higher than that on the first and second floor. The measurement data match the result of FDS simulation. Therefore, the analysis results of the proposed method match well with the calculation results by FDS and can also represent the fire status instantly.

In addition, the analysis and comparison previously described also indicate that the proposed method can be used in practical applications for the risk assessment of building fire and the formulation of an evacuation route. In practical applications, the real-time performance of this method depends on the sensors installed in the building. Data such as temperature and carbon monoxide concentration in each room can be acquired every 2 s. This short time interval of data acquisition ensures

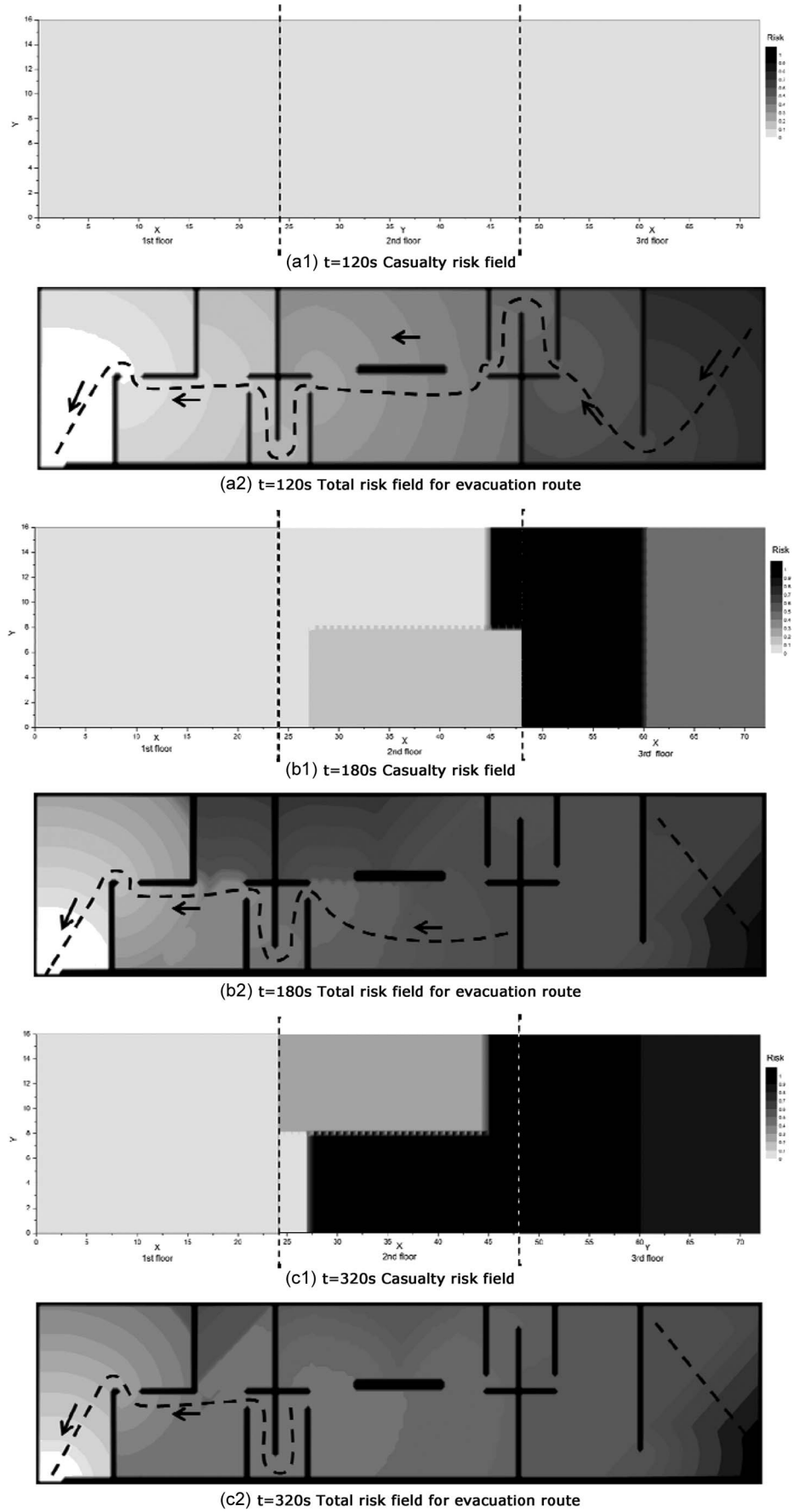

Fig. 6. Results of CR calculation and evacuation route analysis for the real building model. (The second floor is horizontally flipped so that all of the three floors of the building are combined.) (a) $t = 120$ s. (b) $t = 180$ s. (c) $t = 320$ s.

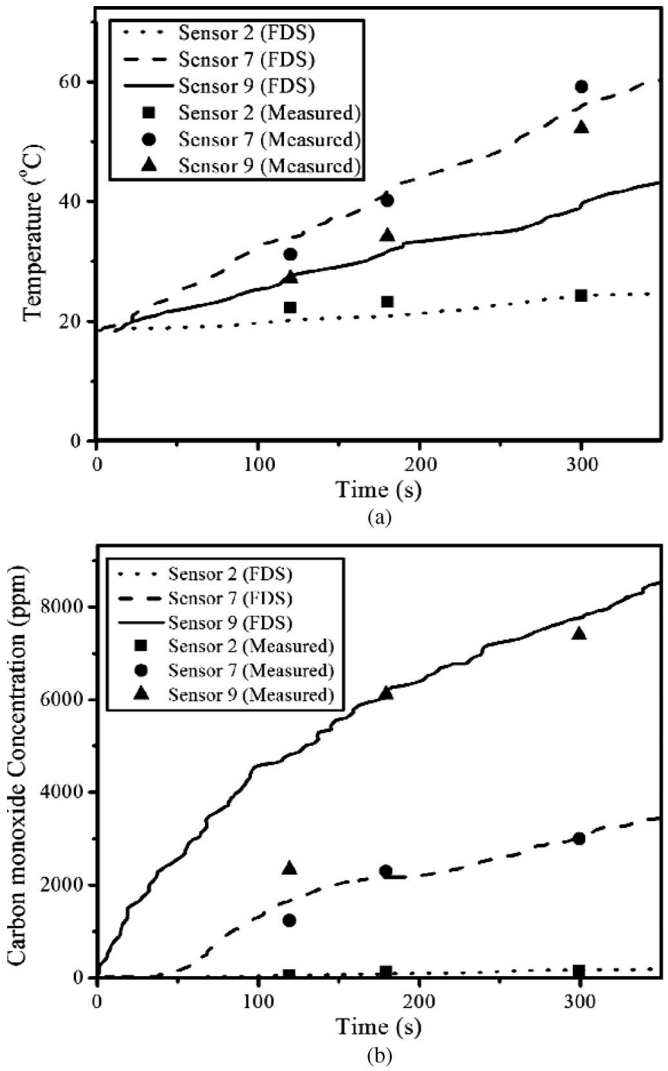

Fig. 7. Comparison on temperature and carbon monoxide concentration of FDS simulation and experiment measured on the three floors in the real building model. (a) Temperature. (b) Carbon monoxide concentration.

the real-time performance of this method. After the data are sent to the computer processor, the program of risk assessment can calculate the risk distribution automatically. Therefore, the analysis result of CR distribution can be updated every 2 s, as does the evacuation route.

In both the numerical and experimental investigations, it is shown that there are still some margins of error by comparing the analysis results with the practical fire status and the assumed fire status. According to error analysis, the causes of errors and uncertainties of the proposed method are listed as follows.

a) In the data acquisition, the sensors are installed on the ceiling of each room. The data acquired by the sensors, including the temperature, the carbon monoxide concentration, the CR, and the total risk fields, are all 2-D. Hence, the temperature and carbon monoxide concentration measured at the install location of the sensors are used for risk calculation. The temperature and carbon monoxide concentration in the height direction are not analyzed in the calculation of the CR distribution and the total risk distribution.

b) As a practical status, there is possibly only one sensor installed in each room in a high-rise building. In the risk calculation of the proposed method, the number of the sensors in each room may directly influence the calculation accuracy of the interpolation calculation. Hence, one sensor is not accurate enough to reflect the distribution of temperature and carbon monoxide concentration in each room, as does the risk distribution. In practical applications, more sensors mean better calculation accuracy.

c) In risk calculation, the harmful effects of high temperature and toxicity of carbon monoxide are uniformly evaluated. The interaction of these two harmful effects is not considered, and the resistibility or robustness of humans is also ignored. Hence, the CR calculated in this paper is not an absolute mortality but a reference value for quantitatively describing and comparing the risk of different places.

Compared with previous works, the method proposed in this paper can instantly evaluate the risk distribution and analysis of the evacuation route during high-rise building fires, based on real-time information on the fire. The applications and investigations show that this method can be used in practical applications. In addition, the analysis result of the risk assessment and the evacuation route formulation will be of great help in real-time evacuation and rescue in high-rise building fires, which are all important in emergency response and safety management.

IV. Conclusion

In this paper, an integrated evacuation route planning method for high-rise building fires has been proposed. This method is composed of real-time data acquisition, risk distribution calculation, and evacuation route formulation. The real-time data acquisition process is achieved by using the sensor system and detectors of temperature and carbon monoxide concentration. The calculation of risk distribution is based on the risk assessment of casualties, including the high temperature and toxicity of carbon monoxide. The formulation of an evacuation route is based on the fast marching level set method, which takes the structure of the building into consideration, particularly for the position of the exit. The acquisition of real-time data of temperature and carbon monoxide concentration is the emphasis of this method that forms the database to evaluate the status and spread of fire. To demonstrate the presented method, a sample building under an assumed fire is used for numerical investigation, and a real building model is used for experimental investigation. In the numerical investigation, the accuracy of the proposed method is tested and verified by comparing the calculation results of this method with FDS. In the experimental investigation, feasibility and practicality is verified by using ten sensors for real-time data acquisition and analysis. In application, sensors may acquire data for risk analysis, and the risk of the whole building can be gained by integrating the risks in all the rooms. The analysis results show that the risk distribution and evacuation route of the building fire can be intuitively displayed. For a different building, the number of the rooms and the complexity of the building structures do

not affect the feasibility of the method, which means that the application of this method does not rely on the spatial layout and building structure. The presented method can be used in practical applications and will be an important technical basis for the program development of rescue and evacuation.

REFERENCES

[1] S. Ge, "High-rise building fire in America," Fire Techn. Products Inform., pp. 79–85, 2011.

[2] A. Shende, M. P. Singh, and P. Kachroo, "Optimization-based feedback control for pedestrian evacuation from an exit corridor," *IEEE Trans. Intell. Transp. Syst.*, vol. 12, no. 4, pp. 1167–1176, Dec. 2011.

[3] S. Xu and H. B.-L. Duh, "A simulation of bonding effects and their impacts on pedestrian dynamics," *IEEE Trans. Intell. Transp. Syst.*, vol. 11, no. 1, pp. 153–161, Mar. 2010.

[4] S. M. Lo, M. Liu, P. H. Zhang, and R. K. K. Yuen, "An artificial neural-network based predictive model for pre-evacuation human response in domestic building fire," *Fire Technol.*, vol. 45, no. 4, pp. 431–449, Dec. 2009.

[5] H. L. Zhu, P. Liu, J.-F. Liu, and X.-L. Tang, "A graph analysis method for abnormal crowd state detection," *Acta Autom. Sin.*, vol. 38, no. 5, pp. 742–750, May 2012.

[6] S. A. Wadoo and P. Kachroo, "Feedback control of crowd evacuation in one dimension," *IEEE Trans. Intell. Transp. Syst.*, vol. 11, no. 1, pp. 182–193, Mar. 2010.

[7] Y.-C. Chiu and P. B. Mirchandani, "Online behavior-robust feedback information routing strategy for mass evacuation," *IEEE Trans. Intell. Transp. Syst.*, vol. 9, no. 2, pp. 264–274, Jun. 2008.

[8] Z. A. Jiang and X. Liu, "Numerical simulation study on high-rise student apartment fire evacuation," *Mater. Sci. Inf. Technol.*, vol. 433–440, pt. 1–8, pp. 3011–3016, 2012.

[9] Z. M. Pei, Z.-D. Deng, S. Xu, and X. Xu, "A new localization method for wireless sensor network nodes based on N-best rank sequence," *Acta Autom. Sin.*, vol. 36, no. 2, pp. 199–207, Feb. 2010.

[10] Y. Peng, Q.-H. Luo, D. Wang, and X.-Y. Peng, "WSN localization method using interval data clustering," *Acta Autom. Sin.*, vol. 38, no. 7, pp. 1190–1199, Jul. 2012.

[11] V. A. Oven and N. Cakici, "Modelling the evacuation of a high-rise office building in Istanbul," *Fire Safety J.*, vol. 44, no. 1, pp. 1–15, Jan. 2009.

[12] S. Gwynne, E. R. Galea, M. Owen, P. J. Lawrence, and L. Filippidis, "A review of the methodologies used in the computer simulation of evacuation from the built environment," *Build. Environ.*, vol. 34, no. 6, pp. 741–749, Nov. 1999.

[13] J. P. Yuan, Z. Fang, Y. C. Wang, S. M. Lo, and P. Wang, "Integrated network approach of evacuation simulation for large complex buildings," *Fire Safety J.*, vol. 44, no. 2, pp. 266–275, Feb. 2009.

[14] A. C. Vrouwenvelder, R. Lovegrove, and M. Holicky, "Risk assessment and risk communication in civil engineering," in *Proc. Safety, Risk Reliab.—Trends Eng.*, 2001, pp. 1–6.

[15] S. N. Jonkman, P. H. van Gelder, and J. K. Vrijling, "An overview of quantitative risk measures for loss of life and economic damage," *J. Hazard. Mater.*, vol. 99, no. 1, pp. 1–30, Apr. 4, 2003.

[16] Y. Yang, A. J. May, and S.-H. Yang, "A generic state model with neighbourhood support from wireless sensor networks for emergency event detection," *Int. J. Emerg. Manag.*, vol. 8, no. 2, pp. 135–152, 2012.

[17] Y. Yanning, A. May, and S.-H. Yang, "Sensor data processing for emergency response," *Int. J. Emerg. Manage.*, vol. 7, no. 3/4, pp. 233–248, Nov./Dec. 2010.

[18] S.-H. Yang and P. Frederick, "SafetyNET—A wireless sensor network for fire protection and emergency responses," *Meas. Control*, vol. 39, no. 7, pp. 218–219, Sep. 2006.

[19] L. M. Sun, *Wireless Sensor Networks*. Beijing, China: Tsinghua Univ. Press, 2005.

[20] D. Cox, E. Jovanov, and A. Milenkovic, "Time synchronization for ZigBee networks," in *Proc. 37th Southeastern Symp. Syst. Theory*, pp. 135–138.

[21] J. Chen, Q. Yu, Y. Zhang, H.-H. Chen, and Y. Sun, "Feedback-based clock synchronization in wireless sensor networks: A control theoretic approach," *IEEE Trans. Veh. Technol.*, vol. 59, no. 6, pp. 2963–2973, Jul. 2010.

[22] P. Yadav, "Cluster based hierarchical wireless sensor networks (CHWSN) and time synchronization in CHWSN," in *Proc. ISCIT*, 2007, pp. 1149–1154.

[23] L. Bernardo, R. Oliveira, M. Pereira, M. Macedo, and P. Pinto, "A wireless sensor MAC protocol for bursty data traffic," in *Proc. IEEE 18th Int. Symp. Pers., Indoor Mobile Radio Commun.*, Jan. 2007, pp. 1–5.

[24] Y. Sun, O. Gurewitz, and D. B. Johnson, "RI-MAC: A receiver-initiated asynchronous duty cycle MAC protocol for dynamic traffic loads in wireless sensor networks," in *Proc. 6th ACM SenSys*, 2008, pp. 1–14.

[25] *Wireless Medium Access Control (MAC) and Physical Layer (PHY) Specifications for Low-Rate Wireless Personal Area Networks (WPANs)*, IEEE Std. 802.15.4-2006, 2006.

[26] *IAR Embedded Workbench IDE User Guide*, 2006.

[27] Z. Y. Han and W. G. Weng, "Comparison study on qualitative and quantitative risk assessment methods for urban natural gas pipeline network," *J. Hazard. Mater.*, vol. 189, no. 1/2, pp. 509–518, May 2011.

[28] Z. Y. Han and W. G. Weng, "An integrated quantitative risk analysis method for natural gas pipeline network," *J. Loss Prev. Process Ind.*, vol. 23, no. 3, pp. 428–436, May 2010.

[29] V. Babrauskas, R. G. Gann, B. C. Levin, M. Paabo, R. H. Harris, R. D. Peacock, and S. Yusa, "A methodology for obtaining and using toxic potency data for fire hazard analysis," *Fire Safety J.*, vol. 31, no. 4, pp. 345–358, Nov. 1998.

[30] M. Kobes, I. Helsloot, B. de Vries, and J. G. Post, "Building safety and human behaviour in fire: A literature review," *Fire Safety J.*, vol. 45, no. 1, pp. 1–11, Jan. 2010.

[31] Z. Y. Han, W. G. Weng, and Q. Y. Huang, "Study on the real-time quantitative risk assessment method of casualty for high-rise building fire," *J. Tsinghua Univ. (Sci. Technol.)*, to be published.

[32] J. A. Sethian, "A fast marching level set method for monotonically advancing fronts," *Proc. Nat. Acad. Sci. USA*, vol. 93, no. 4, pp. 1591–1595, Feb. 1996.

[33] J. A. Sethian, "Fast marching methods," *Siam Rev.*, vol. 41, no. 2, pp. 199–235, Jun. 1999.

[34] J. A. Sethian and D. Adalsteinsson, "An overview of level set methods for etching, deposition, and lithography development," *IEEE Trans. Semicond. Manuf.*, vol. 10, no. 1, pp. 167–184, Feb. 1997.

[35] R. Kimmel and J. A. Sethian, "Computing geodesic paths on manifolds," *Proc. Nat. Acad. Sci. USA*, vol. 95, no. 15, pp. 8431–8435, Jul. 1998.

[36] K. McGrattan, B. Klein, S. Hostikka, and J. Floyd, *Fire Dynamics Simulator (Version5) User's Guide. NIST-SP 1019-5*. Gaithersburg, MD, USA: Nat. Inst. Std. Technol., Jan. 2008.

[37] K. McGrattan, H. Baum, and R. Rehm, *Fire Dynamics Simulator (Version5) Technical Reference Guide. NIST-SP 1018-5*. Gaithersburg, MD: Nat. Inst. Std. Technol, Jan. 2008.

[38] Nat. Inst. Stand. Technol., FDS V5.5, 2010. [Online]. Available: http://fire.nist.gov/fds/

[39] A. H. Rausch, N. A. Eisenberg, and C. J. Lynch, "Continuing development of the vulnerability model (VM2)," Dept. Transp., US Coast Guard, Washington, DC, USA, Tech. Rep. CG-53-77, Feb. 1977.

Zhuyang Han received the B.S. and M.S. degrees in engineering physics from Tsinghua University, Beijing, China, in 2008 and 2010, respectively. He is currently working toward the Ph.D. degree with the Institute of Public Safety Research, Tsinghua University.

His research interests include safety science and risk evaluation, including risk evaluation and evacuation route formation in high-rise building fires, etc.

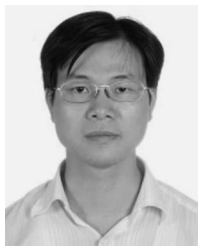

Wenguo Weng received the B.S. degree in engineering thermophysics and the Ph.D. degree in power engineering and engineering thermophysics from the University of Science and Technology of China, Hefei, China, in 1998 and 2004, respectively.

He is currently a Professor with the Institute of Public Safety Research, Department of Engineering Physics, Tsinghua University, Beijing, China. His research interests include evacuation dynamics, fire dynamics, and emergency information systems.

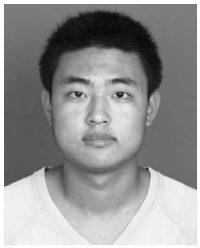

Quanlai Zhao received the B.Eng. degree in safety engineering from China University of Petroleum, Dongying, China, in 2009. He is currently working toward the Ph.D. degree with the Institute of Public Safety Research, Tsinghua University, Beijing, China.

His research interests include fire dynamics, pedestrian control, and path planning.

Xin Ma received the B.S. degree in measuring and control technology from Wuhan University, Wuhan, China, in 2006 and the M.S. degree in automation from Chongqing University of Posts and Telecommunications, Chongqing, China, in 2009. He is currently working toward the Ph.D. degree with the Department of Engineering Physics, Tsinghua University, Beijing, China.

From October 2011 to March 2012, he was an Academic Visitor with the Department of Computer Science, Loughborough University, Leicestershire, U.K. His research interests include wireless communication and public safety risk analysis.

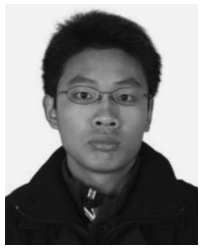

Quanyi Liu received the B.S. degree in fire protection engineering from China University of Mining and Technology, Beijing, China, in 2009. He is currently working toward the Ph.D. degree in nuclear science and technology with the Institute of Public Safety Research, Tsinghua University, Beijing.

His research interests include data analysis and risk analysis.

Quanyi Huang received the B.S. and M.S. degrees in survey engineering and the Ph.D. degree in geodesy and surveying engineering from the School of Geodesy and Geomatics, Wuhan University, Wuhan, China, in 1984, 1987, and 2001, respectively.

He is currently a Professor with the Institute of Public Safety Research, Department of Engineering Physics, Tsinghua University, Beijing, China. In the last five years, he has graduated more than 14 graduate students. His research interests include disaster monitoring and control, comprehensive prediction and warning, multiscale predictive theories and methods, and emergency intelligent decision support technology.

Dr. Huang received the First Prize of the National Science and Technology Award of China in 2011.